

The Fermionic Particle Density of Flat 1+1 Dimensional Spacetime seen by an Arbitrarily Moving Observer.

Carl E. Dolby

Department of Theoretical Physics, 1 Keble Road, Oxford, OX1 3RH, UK

Mark D. Goodsell

Hertford College, Catte Street, Oxford, OX1 3BW, UK

Stephen F. Gull

Astrophysics Group, Cavendish Laboratory, Madingley Road, Cambridge, CB3 0HE, UK

Abstract. A coordinate system is constructed for a general accelerating observer in 1+1 dimensions, and is used to determine the particle density of the massless Dirac vacuum for that observer. Equations are obtained for the spatial distribution and frequency distribution of massless fermions seen by this observer, in terms of the rapidity function of the observer's worldline. Examples that are considered include the uniformly accelerating observer as a limiting case, but do not involve particle horizons. Only the low frequency limit depends on the possible presence of particle horizons. The rest of the spectrum is 'almost thermal' whenever the observer's acceleration is 'almost uniform'.

1. Introduction

Unruh [1] and Davies[2] separately observed in th 1970's that an observer who accelerated uniformly through the Minkowski vacuum would see a "thermal" spectrum of scalar particles, whose perceived temperature depends on the acceleration. The same result holds for fermions [3, 4, 5, 6, 7, 8]. The constant acceleration case has been extensively investigated and reviewed [8, 9]. Most approaches to the constant acceleration case employ Rindler coordinates ([8, 10] are partial exceptions), relying on the symmetry properties of Rindler space, and often emphasizing the importance of the horizon. If the Killing symmetry of Rindler space or its associated horizon were indeed responsible for the result, then questions arise such as: would an observer who accelerates 'almost constantly' see a spectrum of particles which is 'almost thermal'? If an observer's acceleration is constant for a long but finite period of time, will that

observer see an ‘almost thermal’ spectrum during that period? If not, the stability of the Unruh result could be in question.

Evidence from detector models [11, 12] supports the stability of the Unruh result for scalar fields. Sriramkumar [11] demonstrates that a detector which accelerates constantly, but which is turned on only for a finite time, will detect a spectrum of particles differing from the thermal result only by transients.

Bogoliubov approaches to scalar particle creation have been considered in some classes of accelerating frames in 1+1 dimensions [13, 14, 15] and in 3+1 dimensions [16]. The method of Yang et. al. [15] was based on the ‘instantaneous rest frame’ of a given observer. Interesting results were obtained, but their interpretation is limited by the multivalued nature of the instantaneous rest frame [18, 20]. The ‘instantaneous rest frame’ will in general assign more than one time to any event further than $1/g(t)$ from an accelerating observer – it does not *foliate* the spacetime. This leads in [15] to multivalued predictions for the particle content at any such event, raising problems of interpretation. The possible foliations considered in Sanchez [13, 14] and Whiting [16] are similar to those used here, and will be discussed further in the next section.

Below we consider an arbitrarily moving observer in 1+1 dimensions, traveling through the massless fermionic Minkowski vacuum. The foliation we shall use is the “radar time” construction described in full elsewhere [17, 18, 19] and presented briefly in Section 2. In Section 3 this construction is used to derive an expression for the number of fermions measured by this observer in the inertial vacuum, and also the spatial distribution of those fermions. Examples are presented in Section 4, showing that observers who accelerate ‘almost constantly’ see an ‘almost thermal’ spectrum in the causal envelope of their period of acceleration, and further supporting the stability of the Unruh result.

We use “natural” units throughout such that $\hbar = c = 1$, and restrict our study to 1 + 1 dimensions.

2. Radar Coordinates

The concept of radar coordinates for an accelerated observer is not new [18, 21]. They provide a set of coordinates having one-to-one correspondence with the entire region of the Lorentz frame with which the accelerated observer can exchange signals. Consider an observer whose worldline λ in an inertial frame is described by:

$$x^\pm \equiv t \pm x = x_\lambda^\pm(\tau_\lambda) = \int^{\tau_\lambda} d\tau e^{\pm\alpha(\tau)} \quad (1)$$

where τ_λ is the observer’s proper time, and $\alpha(\tau_\lambda)$ is the observer’s ‘rapidity’ at time τ_λ . The exponential $e^{\alpha(\tau_\lambda)}$ is the obvious time-dependent generalization of the k of Bondi’s k -calculus [22, 23, 24]. The observer’s acceleration is $a(\tau_\lambda) = d\alpha/d\tau_\lambda$, and satisfies $a^2 = -A^\mu A_\mu$. The observer’s worldline is completely specified by the choice of origin (i.e. $x^\mu(0)$) and the rapidity function $\alpha(\tau_\lambda)$, or by the choice of origin, the initial velocity, and the function $a(\tau_\lambda)$. The radar time $\tau(x^\mu)$ and radar distance $\rho(x^\mu)$ are defined by:

$$\begin{aligned}\tau &\equiv \frac{1}{2}(\tau^+ + \tau^-) \\ \rho &\equiv \frac{1}{2}(\tau^+ - \tau^-)\end{aligned}\tag{2}$$

where

$\tau^+ \equiv$ time at which a signal from an event travelling in the observer's backward direction (i.e. $t + z = \text{constant}$) is received or sent.

$\tau^- \equiv$ time at which a signal travelling in the observer's forward direction (i.e. $t - z = \text{constant}$) is received or sent.

and are such that ρ is positive in the observer's forward direction and negative behind – this choice is convenient for 1 + 1 dimensions. From equations (1) and (2) it follows that τ^\pm are related to x^\pm by

$$x^\pm = x_\lambda^\pm(\tau^\pm)$$

To see the connection between the τ , ρ coordinates used here, and the t' , x' used in the scalar field work of Sanchez and Whiting [13, 14, 16], consider the most general transformation, written as equation (6.2) of [14] and described briefly in [16]. This is of the form:

$$x^+ = g(x'^+) \text{ and } x^- = -f(-x'^-)\tag{3}$$

where f and g are analytic functions and $x'^\pm = t' \pm x'$ are the ‘accelerated coordinates’. The coordinate t' in general has no connection with the proper time of any particular observer. In radar coordinates, the line $\rho = 0$ is the worldline of the observer. The requirement that τ coincide with the observer's proper time on this worldline gives:

$$\frac{dx_\lambda^+}{d\tau} \frac{dx_\lambda^-}{d\tau} = 1\tag{4}$$

It is this condition that uniquely assigns the choice of foliation to the choice of observer, and which allows $x_\lambda^\pm(\tau)$ to be written in terms of the observer's rapidity function, as in equation (1). Throughout [13], and in the main body of [14, 16], attention is restricted to the case $f = g$. Combined with the restriction (4), this leads to the time-reversal invariant case considered at the end of Section 3.

The metric in radar coordinates is:

$$ds^2 = e^{(\alpha(\tau^+) - \alpha(\tau^-))} (d\tau^2 - d\rho^2)$$

The ‘time-translation vector field’ [17, 19] is simply $k^\mu \frac{\partial}{\partial x^\mu} = \frac{\partial}{\partial \tau}$, and the hypersurfaces Σ_τ are hypersurfaces of constant τ . To illustrate these definitions we consider some examples.

2.1. Inertial Observer

As a consistency check, consider an inertial observer with a velocity v relative to our original frame. Then α is constant, and $x_\lambda^\pm(\tau_\lambda) = e^{\pm\alpha}\tau_\lambda$. The coordinates τ^\pm are now given by $\tau^\pm = e^{\mp\alpha}x^\pm$, so that

$$\tau = \frac{1}{2}(e^{-\alpha}x^+ + e^{\alpha}x^-) = \frac{t - vx}{\sqrt{1 - v^2}}, \quad \rho = \frac{1}{2}(e^{-\alpha}x^+ - e^{\alpha}x^-) = \frac{x - vt}{\sqrt{1 - v^2}}$$

The radar coordinates of an inertial observer are just the coordinates of that observer's rest frame, as expected.

2.2. Constant Acceleration

The simplest nontrivial case is that of constant acceleration [20]. In this case $\alpha(\tau) = a\tau$ and we have $x_\lambda^\pm(\tau_\lambda) = \pm a^{-1}e^{\pm a\tau_\lambda}$, which gives:

$$\tau = \frac{1}{2a} \log \left(\frac{x+t}{x-t} \right) \quad \rho = \frac{1}{2a} \log (a^2(x^2 - t^2)) \quad (5)$$

$$ds^2 = e^{2a\rho}(d\tau^2 - d\rho^2) \quad (6)$$

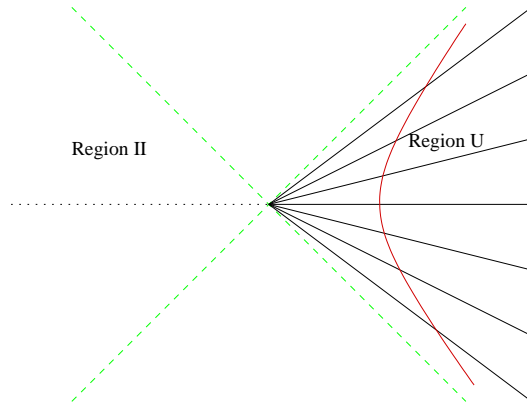


Figure 1. Hypersurfaces of simultaneity of a uniformly accelerating observer.

These are Rindler coordinates, which cover only region U of Figure 1, as expected [18, 21]. The hypersurfaces of constant τ are given by $t_{\tau_0}(x) = x \tanh(a\tau_0)$.

2.3. The ‘Smooth Turnaround’ Observer

Consider an observer (Alice say) with $\alpha(\tau_\lambda) = a\tau_c \tanh(\tau/\tau_c)$. Her trajectory is given by:

$$x_\lambda^\pm(\tau_\lambda) = \int_0^{\tau_\lambda} d\tau e^{\pm a\tau_c \tanh(\tau/\tau_c)}$$

She has acceleration $a(\tau) = a \cosh^{-2}(\tau/\tau_c)$, so is uniformly accelerating for $|\tau| \ll \tau_c$ and is inertial for $|\tau| \gg \tau_c$. As the parameter $\tau_c \rightarrow \infty$ this case approaches the constant-acceleration case. However, there are no horizons for this ‘smooth-turnaround’ observer.

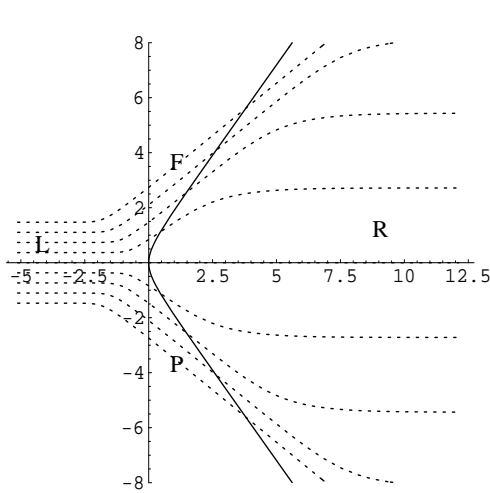


Figure 2(A). Hypersurfaces of simultaneity for the ‘smooth turnaround’ observer in the (x, t) plane (in units of $1/a$) for $\tau_c = 1/a$.

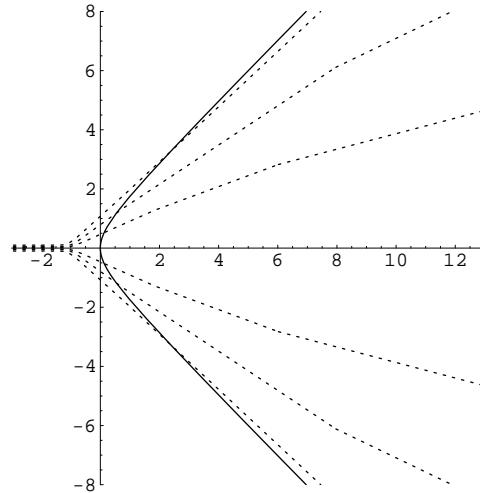


Figure 2(B). Hypersurfaces of simultaneity for the ‘smooth turnaround’ observer, in the (x, t) plane (in units of $1/a$) for $\tau_c = 3/a$.

Figure 2 shows the hypersurfaces of constant τ for a smooth-turnaround observer (in units of $1/a$) for $\tau_c = 1/a$ (A) and $3/a$ (B). In Figure 2 (A), in which the turn-around time is relatively short, we can distinguish four regions. In region F, where Alice is effectively inertial with velocity $\tanh(a\tau_c)$, her hypersurfaces of ‘simultaneity’ are those appropriate to her status as an inertial observer. The same applies in region P. In regions L, R however, her hypersurfaces of simultaneity are flat, and are contracted/expanded by the Doppler factors $e^{a\tau_c}$ and $e^{-a\tau_c}$ respectively. This prevents the multi-valuedness of the ‘instantaneous rest frame’ construction [23, 24, 15]. (The point is discussed further in [18], in the context of the relativistic “twin-paradox”.) Figure 2 (B) is dominated by the period of acceleration, and bears closer resemblance to the constant acceleration case of Figure 1.

2.4. Acceleration at Late Times

Consider an observer (Bob say) with

$$\alpha(\tau_\lambda) = a\tau_c \log(1 + e^{\tau_\lambda/\tau_c}) \quad (7)$$

His acceleration is:

$$a(\tau_\lambda) = \frac{a}{1 + e^{-\tau_\lambda/\tau_c}} \quad (8)$$

Bob is stationary at early times, and his acceleration approaches a at late times. Bob’s hypersurfaces of simultaneity are shown in Figure 3 (A) (in units of $1/a$) for $\tau_c = 1/a$. There is a future horizon at $x^- = \int_0^\infty d\tau (1 + e^{\tau/\tau_c})^{-a\tau_c}$, but no past horizon.

Regions L, F are narrow in Figure 3 (A), and are bounded by the horizon. In the (ρ, τ) plane, however, describing the space seen by the observer, the horizon is of course not visible (it corresponds to $\tau^- \rightarrow \infty$ for constant τ^+), and the L,F regions

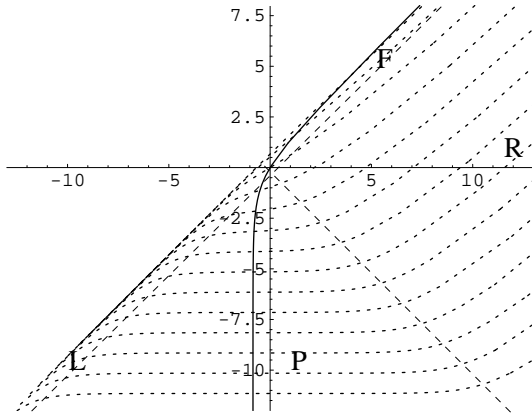


Figure 3(A). Hypersurfaces of simultaneity for an observer who accelerates at late times, in the (x, t) plane (in units of $1/a$) for $\tau_c = 1/a$.

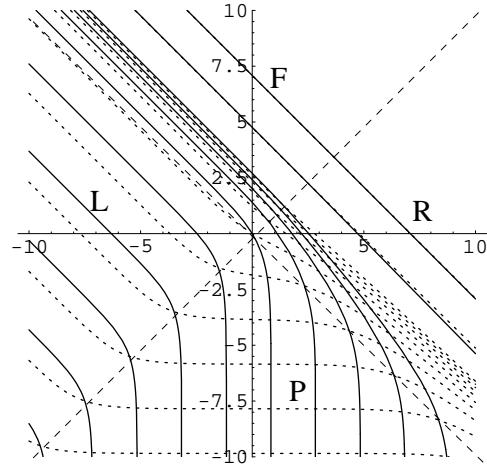


Figure 3(B). Hypersurfaces of constant t (dotted) and constant x (hard) in the (ρ, τ) plane (in units of $1/a$) of an observer who accelerates at late times, for $\tau_c = 1/a$.

are infinite in extent. This can be seen in Figure 3 (B), where surfaces of constant t (dotted) and constant x (hard) are plotted in the (ρ, τ) plane. The values of t, x shown are $\{-10, -8, -6, -4, -2, 0, 2, 4, 6, 8, 60, 600\}$ in units of $1/a$. The line $x = 600/a$ (top right) almost coincides with the line $t = 600/a$, each being almost null. The same applies to the lines $x = 60/a$ and $t = 60/a$. All of the (ρ, τ) plane is covered by (x, t) , although the lines of constant x (or of constant t) become exponentially tightly packed in regions F and R. The future horizon of Figure 3 (A) implies in Figure 3 (B) that the $x = -4/a$ line (for instance) never crosses the $t = -2/a$ line in the (ρ, τ) plane. The point $(x, t) = (-4/a, -2/a)$ is outside the observer's causal envelope.

3. Particle Density of the Dirac Vacuum

The massless Dirac equation in flat 1 + 1 dimensional space can be written

$$\gamma^\mu \frac{\partial \psi}{\partial x^\mu} = 0 \quad (9)$$

and is frame-invariant provided that the γ^μ -matrices transform as (contravariant) vectors. By choosing the flat-space Dirac matrices $\bar{\gamma}^0 = \begin{pmatrix} 0 & 1 \\ 1 & 0 \end{pmatrix}$ and $\bar{\gamma}^1 = \begin{pmatrix} 0 & -1 \\ 1 & 0 \end{pmatrix}$ (which satisfy $\{\bar{\gamma}^\mu, \bar{\gamma}^\nu\} = 2\eta^{\mu\nu}$) and introducing the basis spinors $\phi_+ = \begin{pmatrix} 1 \\ 0 \end{pmatrix}$, $\phi_- = \begin{pmatrix} 0 \\ 1 \end{pmatrix}$, we can write the general solution as

$$\psi = \psi_+(x^-)\phi_+ + \psi_-(x^+)\phi_- \quad (10)$$

To define the (inertial) Minkowski vacuum, introduce the plane wave basis:

$$u_{p,F,\pm} = e^{\mp i p x^-} \phi_\pm, \quad u_{p,B,\pm} = e^{\mp i p x^+} \phi_\pm \quad \text{for } p > 0 \quad (11)$$

These modes are normalized to $2\pi\delta(p' - p)$, and have been decoupled into “forward-moving” modes (denoted with a subscript “F”), and “backward-moving” modes (with subscript “B”).

The Dirac field operator $\hat{\psi}(x)$ can now be written:

$$\hat{\psi}(x) = \int_0^\infty \frac{dp}{2\pi} \sum_{\sigma=F,B} \{u_{p,\sigma,+}a_{p,\sigma} + u_{p,\sigma,-}b_{p,\sigma}^\dagger\} \quad (12)$$

and the Dirac vacuum $|0_M\rangle$ can be defined by the condition $a_{p,\sigma}|0_M\rangle = 0 = b_{p,\sigma}|0_M\rangle$ for all p, σ .

Consider now an arbitrarily moving observer, with coordinates (τ, ρ) . With $\gamma^0 = \frac{\partial\tau}{\partial t}\bar{\gamma}^0 + \frac{\partial\tau}{\partial z}\bar{\gamma}^1$ and $\gamma^1 = \frac{\partial\rho}{\partial t}\bar{\gamma}^0 + \frac{\partial\rho}{\partial z}\bar{\gamma}^1$, equation (9) becomes

$$g^{00}\frac{\partial\psi}{\partial\tau} = -\gamma^0\gamma^1\frac{\partial\psi}{\partial\rho}$$

Since $\gamma^0\gamma^1 = g^{00}\bar{\gamma}^0\bar{\gamma}^1$, this can be written as

$$i\frac{\partial\psi}{\partial\tau} = -i\bar{\gamma}^0\bar{\gamma}^1\frac{\partial\psi}{\partial\rho} \equiv \hat{H}_{nh}\psi \quad (13)$$

Following [19, 25] we construct particle/antiparticle modes for this observer, by diagonalising the ‘second quantized’ Hamiltonian:

$$\hat{H}(\tau) = \int_{\Sigma_\tau} \sqrt{-g}T_{\mu\nu}(\hat{\psi}(x))k^\mu d\Sigma^\nu \quad (14)$$

$$= \frac{i}{2} \int \left(\hat{\psi}^\dagger M \frac{\partial\hat{\psi}}{\partial\tau} - \frac{\partial\hat{\psi}^\dagger}{\partial\tau} M \hat{\psi} \right) d\rho \quad (15)$$

$$\text{where } M = \sqrt{-g}\bar{\gamma}^0\gamma^0 = \frac{1}{2} \left[e^{-\alpha(\tau^-)}(\mathbb{I} + \bar{\gamma}^0\bar{\gamma}^1) + e^{\alpha(\tau^+)}(\mathbb{I} - \bar{\gamma}^0\bar{\gamma}^1) \right] \quad (16)$$

We now seek the spectrum of the ‘first quantized’ Hamiltonian $\hat{H}_1(\tau) = \frac{1}{2}(\hat{H}_{nh} + \hat{H}_{nh}^\dagger)$, which acts on states defined on Σ_τ . The inner product expressed on such hypersurfaces can be written in radar coordinates as:

$$\langle\psi|\phi\rangle_{\Sigma_{\tau_0}} = \int_{-\infty}^{\infty} d\rho \sqrt{-g}\psi^\dagger\bar{\gamma}^0\gamma^0\phi = \int_{-\infty}^{\infty} d\rho \psi^\dagger M\phi \quad (17)$$

To deduce \hat{H}_{nh}^\dagger , consider

$$\begin{aligned} \langle\hat{H}_{nh}\psi|\phi\rangle_{\Sigma_{\tau_0}} &= \frac{1}{2} \int_{-\infty}^{\infty} d\rho \left(\hat{H}_{nh}\psi \right)^\dagger M\phi \\ &= \langle\psi| -i\sigma\frac{\partial}{\partial\rho}|\phi\rangle_{\Sigma_{\tau_0}} - \int_{-\infty}^{\infty} d\rho \psi^\dagger M \left(M^{-1}i\sigma\frac{\partial M}{\partial\rho} \right) \phi \end{aligned} \quad (18)$$

where we have discarded surface terms at $\rho \rightarrow \pm\infty$, and have assumed that the functions U^+ and U^- are continuous. This gives our Hermitian Hamiltonian \hat{H}_1 as

$$\begin{aligned} \hat{H}_1(\tau_0) = & -i\sigma \frac{\partial}{\partial \rho} \\ & + \frac{i}{4} [a(\tau_0 + \rho)(\mathbb{I} - \bar{\gamma}^0 \bar{\gamma}^1) - a(\tau_0 - \rho)(\mathbb{I} + \bar{\gamma}^0 \bar{\gamma}^1)] \end{aligned} \quad (19)$$

The positive/negative eigenstates of this Hamiltonian will determine the particle/antiparticle content of the Minkowski vacuum measured by our accelerated observer.

By writing these eigenstates as $\psi_{\tau_0} = f_+ \phi_+ + f_- \phi_-$, equation (19) gives

$$\begin{aligned} \omega f_+ = & -i \frac{\partial f_+}{\partial \rho} - \frac{i}{2} a(\tau_0 - \rho) f_+ \\ \omega f_- = & i \frac{\partial f_-}{\partial \rho} + \frac{i}{2} a(\tau_0 + \rho) f_- \end{aligned} \quad (20)$$

and since $\left(\frac{\partial}{\partial \rho}\right)_\tau = \left(\frac{\partial}{\partial \tau^+}\right)_\tau = -\left(\frac{\partial}{\partial \tau^-}\right)_\tau$, these equations can be rewritten as

$$\begin{aligned} \omega f_+ = & i \frac{df_+}{d\tau^-} - \frac{i}{2} a(\tau^-) f_+ \\ \omega f_- = & i \frac{df_-}{d\tau^+} + \frac{i}{2} a(\tau^+) f_- \end{aligned} \quad (21)$$

with solutions

$$\begin{aligned} f_+ = & A_\omega e^{\alpha(\tau^-)/2} e^{-i\omega\tau^-} \\ f_- = & B_\omega e^{-\alpha(\tau^+)/2} e^{-i\omega\tau^+} \end{aligned} \quad (22)$$

where A_ω and B_ω are normalisation constants. Comparison with equation (10) (and observing that τ^+ is a function of x^+ , τ^- a function of x^-) reveals that in (21) we have found not only eigenstates on Σ_τ , but have derived solutions to the Dirac equation (9) which are eigenstates for all τ . This is in general only possible for the massless case, and is a consequence of conformal invariance. By choosing $\{A = 1, B = 0\}$ and $\{A = 0, B = 1\}$ respectively, we can define ‘‘forward-moving’’ and ‘‘backward-moving’’ modes:

$$\psi_{\omega,F,\pm} = e^{\alpha(\tau^-)/2} e^{\mp i\omega\tau^-} \phi_+, \quad \psi_{\omega,B,\pm} = e^{-\alpha(\tau^+)/2} e^{\mp i\omega\tau^+} \phi_- \quad \text{for } \omega > 0 \quad (23)$$

These are ‘normalized’ to $2\pi\delta(\omega - \omega')$ with respect to (17), but are not yet defined in general over the whole spacetime. We wish to write the field operator $\hat{\psi}(x)$ in terms of these modes as:

$$\hat{\psi}(x) = \hat{\psi}^{(+)}(x) + \hat{\psi}^{(-)}(x) + \hat{\psi}^{(0)}(x) \quad (24)$$

where

$$\begin{aligned} \hat{\psi}^{(+)}(x) & \equiv \int \frac{d\omega}{2\pi} \sum_{\sigma=F,B} \psi_{\omega,\sigma,+} \tilde{a}_{\omega,\sigma} \\ \hat{\psi}^{(-)}(x) & \equiv \int \frac{d\omega}{2\pi} \sum_{\sigma=F,B} \psi_{\omega,\sigma,-} \tilde{b}_{\omega,\sigma}^\dagger \end{aligned} \quad (25)$$

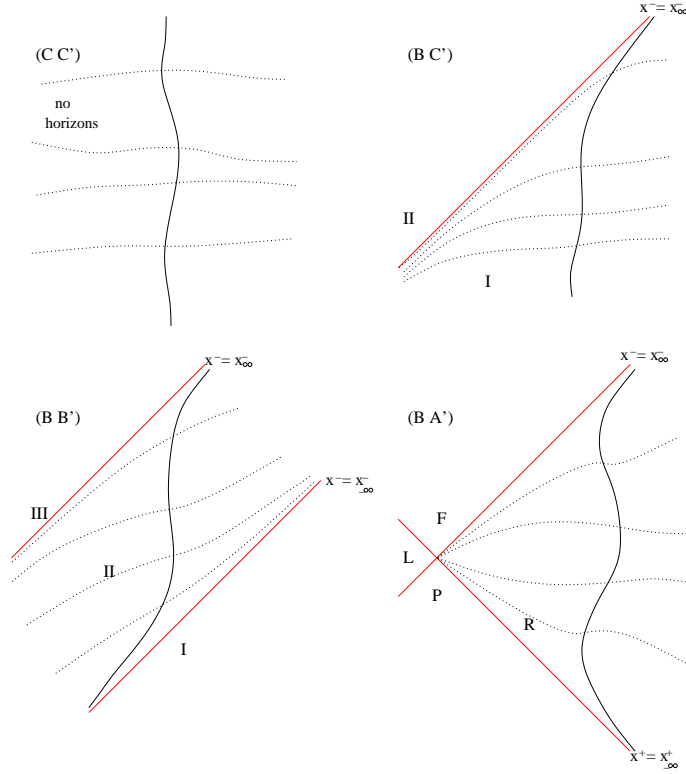


Figure 4. Representation of four of the nine possibilities for the structure of the causal envelope of an observer in 1+1 dimensional flat space. The dark curved lines represent a typical observer from each class, and the dotted lines represent typical ‘hypersurfaces of simultaneity’ for such observers.

and $\hat{\psi}^{(0)}(x)$ has compact support outside the causal envelope of our observer. To describe this construction, acceleration horizons must be considered. Consider the behavior of $x^{\pm}(\tau_{\lambda})$ as $\tau_{\lambda} \rightarrow \infty$. There are three possibilities:

$$x^{+}(\tau_{\lambda}) \rightarrow x_{\infty}^{+} < \infty \quad \text{and} \quad x^{-}(\tau_{\lambda}) \rightarrow \infty \quad (\text{A})$$

$$x^{-}(\tau_{\lambda}) \rightarrow x_{\infty}^{-} < \infty \quad \text{and} \quad x^{+}(\tau_{\lambda}) \rightarrow \infty \quad (\text{B})$$

$$x^{+}(\tau_{\lambda}) \rightarrow \infty \quad \text{and} \quad x^{-}(\tau_{\lambda}) \rightarrow \infty \quad (\text{C})$$

(x_{∞}^{\pm} cannot both be finite, since $\frac{dx^{+}}{d\tau_{\lambda}} \frac{dx^{-}}{d\tau_{\lambda}} = 1$ for all τ_{λ}). Similarly, as $\tau_{\lambda} \rightarrow -\infty$ we have the possibilities

$$x^{+}(\tau_{\lambda}) \rightarrow x_{-\infty}^{+} > -\infty \quad \text{and} \quad x^{-}(\tau_{\lambda}) \rightarrow -\infty \quad (\text{A}')$$

$$x^{-}(\tau_{\lambda}) \rightarrow x_{-\infty}^{-} > -\infty \quad \text{and} \quad x^{+}(\tau_{\lambda}) \rightarrow -\infty \quad (\text{B}')$$

$$x^{+}(\tau_{\lambda}) \rightarrow -\infty \quad \text{and} \quad x^{-}(\tau_{\lambda}) \rightarrow -\infty \quad (\text{C}')$$

These combine to give nine possible structures of the causal envelope of the observer. We consider four of these cases here (the other five are similar):

- (C C') There are no horizons in this case. It is easy to see that the modes $\psi_{\omega, \sigma, \pm}$ are complete, so that we can achieve (24) with $\hat{\psi}^{(0)}(x) = 0$.

- (B C') In this case there is a future acceleration horizon at $x^- = x_\infty^-$, which separates the spacetime into two regions – denoted I and II. Region I is the causal envelope of the observer, and region II the remainder. The backward-moving modes are defined naturally on the whole spacetime, since they are functions of x^+ only (the range of $x^+(\tau_\lambda)$ covers the whole real line). They form a complete set of backward moving modes. Although they were normalized on a hypersurface which is not Cauchy, it is straightforward to verify that the same norm holds on any Cauchy surface. The forward moving modes, on the other hand, are defined only in Region I. They can be extended to the whole spacetime by specifying $\psi_{\omega,F,\pm}(x) = 0$ throughout region II. This ensures that the Dirac equation is satisfied even on the horizon (a wave-packet formed from these will be continuous on the horizon) and ensures that they are normalized to $(2\pi)\delta(\omega - \omega')$ on any Cauchy surface. Although they do not form a complete set, they can easily be supplemented by further ‘forward moving modes’, $\psi_{i,II}(x)$, which are zero outside region II, and which together with the $\{\psi_{\omega,F,\pm}(x)\}$ comprise a complete set. (The $\psi_{i,II}(x)$ might be chosen to be the forward moving modes of an observer in Case (C B'), which has x_∞^- as a past horizon.) We can then achieve (24) with

$$\hat{\psi}^{(0)}(x) = \sum_i \psi_{i,II}(x)c_i$$

where the operators c_i satisfy anticommutation relations appropriate to the normalization of the ψ_i . There is considerable freedom in choosing these modes, which do not appear in the Hamiltonian $\hat{H}(\tau)$ (they all satisfy $\hat{H}_1\psi_{i,II} = 0$) or in the number density operator $\hat{N}(x)$ (defined below) for this observer. These modes are ‘unobservable’ by our present observer, since they vanish throughout the corresponding causal envelope.

- (B B') In this case there are future and past acceleration horizons at $x^- = x_{\pm\infty}^-$, which divide the spacetime into regions I, II and III as shown in Figure 4. The backward-moving modes again form a complete set, defined on the whole spacetime. The forward-moving modes can be extended by specifying $\psi_{\omega,F,\pm}(x) = 0$ throughout regions I and III. They may be supplemented to form a complete set by including modes $\{\psi_{i,I}(x)\}$ and $\{\psi_{i',III}(x)\}$, with compact support in regions I and III respectively. Equation (24) is then achieved with

$$\hat{\psi}^{(0)}(x) = \sum_i \psi_{i,I}(x)c_{i,I} + \sum_{i'} \psi_{i',III}(x)c_{i',III}$$

- (B A') This includes the well-studied uniform acceleration case (Section 2.2). It involves a future horizon at $x^- = x_\infty^-$ and a past horizon at $x^+ = x_{-\infty}^+$, which intersect at a point, and divide the spacetime into 4 regions, denoted L, R, F and P in Figure 4. All hypersurfaces Σ_τ terminate at this point of intersection. In this case the backward-moving modes are defined in Regions R and F, and can be extended to the whole spacetime by specifying $\psi_{\omega,B,\pm}(x) = 0$ throughout regions L and P. They then satisfy $\langle \psi_{\omega',B,\lambda'} | \psi_{\omega,B,\lambda} \rangle = (2\pi)\delta_{\lambda\lambda'}\delta(\omega - \omega')$ on any Cauchy

surface. They can be supplemented by backward-moving modes $\psi_{i,LP}(x)$ having compact support in the union of Regions L and P. The forward-moving modes can be similarly extended, and supplemented by modes $\psi_{i',LF}(x)$ having compact support in the union of Regions L and F. Equation (24) is then achieved with

$$\hat{\psi}^{(0)}(x) = \sum_i \psi_{i,LP}(x) c_{i,LP} + \sum_{i'} \psi_{i',LF}(x) c_{i',LF}$$

Equation (24) has now been confirmed in all cases, and it is routine to substitute $\hat{\psi}(x)$ into equation (15) to obtain the (pre-normal-ordered) Hamiltonian:

$$\hat{H}(\tau) = \int \frac{d\omega}{2\pi} \omega \sum_{\sigma=F,B} \{ \tilde{a}_{\omega,\sigma}^\dagger \tilde{a}_{\omega,\sigma} - \tilde{b}_{\omega,\sigma} \tilde{b}_{\omega,\sigma}^\dagger \} \quad (26)$$

which has successfully been diagonalised, and does not depend on $\hat{\psi}^{(0)}(x)$. The time-independence of the operators $\tilde{a}_{\omega,\sigma}, \tilde{b}_{\omega,\sigma}$ and of the Hamiltonian $\hat{H}(\tau)$ follows because the solutions $\psi_{\omega,\sigma,\pm}(x)$ are eigenstates of $\hat{H}_1(\tau)$ for all τ (and with the same eigenvalue ω for all τ).

The (second-quantized) total number operator $\hat{N}(\tau)$ [19, 25] can be written in terms of particle/antiparticle density operators $\hat{N}^\pm(x)$ as

$$\hat{N}(\tau) = \hat{N}^+ + \hat{N}^- = \int_{-\infty}^{\infty} d\rho (\hat{N}^+(x) + \hat{N}^-(x)) \quad (27)$$

$$\text{where } \hat{N}^+(x) = \hat{\psi}^{(+)\dagger}(x) M \hat{\psi}^{(+)}(x) \quad (28)$$

$$= \int_0^\infty \frac{d\omega}{2\pi} \int_0^\infty \frac{d\omega'}{2\pi} \{ e^{i(\omega'-\omega)\tau^-} \tilde{a}_{\omega',F}^\dagger \tilde{a}_{\omega,F} + e^{i(\omega'-\omega)\tau^+} \tilde{a}_{\omega',B}^\dagger \tilde{a}_{\omega,B} \} \quad (29)$$

$$= \hat{N}_F^+(\tau^-) + \hat{N}_B^+(\tau^+) \quad (30)$$

$$\text{(say), and } \hat{N}^-(x) = - : \hat{\psi}^{(-)\dagger}(x) M \hat{\psi}^{(-)}(x) : \quad (31)$$

$$= \int_0^\infty \frac{d\omega}{2\pi} \int_0^\infty \frac{d\omega'}{2\pi} \{ e^{i(\omega'-\omega)\tau^-} \tilde{b}_{\omega',F}^\dagger \tilde{b}_{\omega,F} + e^{i(\omega'-\omega)\tau^+} \tilde{b}_{\omega',B}^\dagger \tilde{b}_{\omega,B} \} \quad (32)$$

$$= \hat{N}_F^-(\tau^-) + \hat{N}_B^-(\tau^+) \quad (33)$$

where the normal ordering is with respect to the observer's particle interpretation (i.e. the $\tilde{b}_{\omega,F}$). By equating expressions (12) and (24) for $\hat{\psi}(x)$, we find that

$$\tilde{a}_{\omega,\sigma} = \int_0^\infty \frac{dp}{2\pi} \{ \langle \psi_{\omega,\sigma,+} | u_{p,\sigma,+} \rangle a_{p,\sigma} + \langle \psi_{\omega,\sigma,+} | u_{p,\sigma,-} \rangle b_{p,\sigma}^\dagger \} \quad (34)$$

$$\tilde{b}_{\omega,\sigma} = \int_0^\infty \frac{dp}{2\pi} \{ \langle \psi_{\omega,\sigma,-} | u_{p,\sigma,+} \rangle^* a_{p,\sigma}^\dagger + \langle \psi_{\omega,\sigma,-} | u_{p,\sigma,-} \rangle^* b_{p,\sigma} \} \quad (35)$$

(A similar expression exists for the \tilde{c}_i .) Substitution into \hat{N}^\pm allows us to evaluate the particle content of the Dirac Vacuum $|0_M\rangle$ as measured by this observer. For instance, the total number of particles/antiparticles measured is:

$$\begin{aligned}
 N^+ &= \langle 0_M | \hat{N}^+ | 0_M \rangle = \int_0^\infty \frac{d\omega}{2\pi} \sum_{\sigma=F,B} (\beta\beta^\dagger)_{\omega\omega,\sigma} \\
 N^- &= \langle 0_M | \hat{N}^- | 0_M \rangle = \int_0^\infty \frac{d\omega}{2\pi} \sum_{\sigma=F,B} (\gamma\gamma^\dagger)_{\omega\omega,\sigma}
 \end{aligned} \tag{36}$$

where

$$\begin{aligned}
 \beta_{\omega p, F} &\equiv \langle \psi_{\omega, F, +} | u_{p, F, -} \rangle = \int_{-\infty}^\infty d\rho e^{-\alpha(\rho)/2} e^{i\omega\rho} e^{ipx_\lambda^-(\rho)} \\
 \beta_{\omega p, B} &\equiv \langle \psi_{\omega, B, +} | u_{p, B, -} \rangle = \int_{-\infty}^\infty d\rho e^{\alpha(\rho)/2} e^{i\omega\rho} e^{ipx_\lambda^+(\rho)}
 \end{aligned} \tag{37}$$

$$\text{and } \gamma_{\omega p, \sigma} \equiv \langle \psi_{\omega, \sigma, -} | u_{p, \sigma, +} \rangle = \beta_{\omega p, \sigma}^* \tag{38}$$

Here $\beta_{\omega p, \sigma}$ and $\gamma_{\omega p, \sigma}$ are independent of τ , since the states $\psi_{\omega, \sigma, \pm}$ are all solutions of the Dirac equation. The variable ρ serves simply as an integration dummy. Though its physical origins come from an integral over space we could equally well use the label τ_λ , viewing the integral as an integral along the observer's worldline.

From equation (38) we see that $(\gamma\gamma^\dagger)_{\omega\omega, \sigma} = (\beta\beta^\dagger)_{\omega\omega, \sigma}$ for both σ , so that from (36) the total number and frequency distribution of 'forward'-moving particles are equal to those of 'forward'-moving antiparticles, and similarly for 'backward'-moving particles. In general, the forward-moving particle content need not resemble the backward-moving particle content.

The formula for the distribution of particles also takes a simple form:

$$\begin{aligned}
 n_F^+(\tau, \rho) &\equiv \langle 0_M | \hat{N}_F^+(x) | 0_M \rangle = \int_0^\infty \frac{d\omega}{2\pi} \int_0^\infty \frac{d\omega'}{2\pi} (\beta\beta^\dagger)_{\omega\omega', F} e^{i(\omega' - \omega)\tau^-} \\
 n_F^-(\tau, \rho) &\equiv \langle 0_M | \hat{N}_F^-(x) | 0_M \rangle = \int_0^\infty \frac{d\omega}{2\pi} \int_0^\infty \frac{d\omega'}{2\pi} (\gamma\gamma^\dagger)_{\omega\omega', F} e^{-i(\omega' - \omega)\tau^-}
 \end{aligned} \tag{39}$$

$$= n_F^+(\tau, \rho) \tag{40}$$

where equation (38) has been used to reach the last line. The spatial distributions of particles and antiparticles are the same, as expected from local conservation of charge. Further, the integral over $p > 0$ which is implicit in the definition of $(\beta\beta^\dagger)_{\omega\omega', \sigma}$ can be evaluated explicitly to yield:

$$(\beta\beta^\dagger)_{\omega\omega', F} = \frac{2}{\pi} \int_{-\infty}^\infty d\tau_a e^{-2i\omega_d\tau_a} \int_0^\infty d\tau_d \sin(2\omega_a\tau_d) g_+(\tau_a, \tau_d) \tag{41}$$

$$\text{where } \omega_a = \frac{1}{2}(\omega + \omega') \quad \omega_d = \frac{1}{2}(\omega' - \omega) \tag{42}$$

$$\text{and } g_\pm(\tau_a, \tau_d) = \frac{1}{2\tau_d} - \frac{\exp[\mp\frac{1}{2}(\alpha(\tau_a + \tau_d) + \alpha(\tau_a - \tau_d))]}{\int_{-\tau_d}^{\tau_d} d\tau \exp[\mp\alpha(\tau_a + \tau)]} \tag{43}$$

In equation (39) this yields:

$$n_F^\pm(\tau^-) = \frac{1}{4\pi^2} \int_{-\infty}^{\infty} \frac{d\tau}{\tau} g_+(\tau^- + \tau, \tau) = \int_0^{\infty} \frac{d\omega_a}{2\pi} n_{F,\omega}(\tau^-) \quad (44)$$

where

$$n_{F,\omega}(\tau^-) = \frac{2}{\pi^2} \int_{-\infty}^{\infty} d\tau_a \frac{\sin[2\omega(\tau^- - \tau_a)]}{\tau^- - \tau_a} \int_0^{\infty} d\tau_d \sin(2\omega\tau_d) g_+(\tau_a, \tau_d) \quad (45)$$

This density is a function only of $\tau^- = \tau - \rho$, as expected for forward-moving massless particles. It is defined such that $n_F^\pm(\tau^-) d\rho$ gives the number of particles within $d\rho$ of the point (τ, ρ) . Integration of $n_{F,\omega}(\tau^-)$ over ρ at any time τ gives the total number of forward-moving particles of frequency ω :

$$(\beta\beta^\dagger)_{\omega\omega,F} = \int_{-\infty}^{\infty} d\rho n_{F,\omega}(\tau^-) = \int_{-\infty}^{\infty} d\tau^- n_{F,\omega}(\tau^-) \quad (46)$$

In combination with equation (44), this result suggests that $n_{F,\omega}(\tau^-)$ should be interpreted as the frequency distribution of forward moving particles/antiparticles at the point τ^- . Though this interpretation is reasonable, $n_{F,\omega}(\tau^-)$ must be averaged over a suitable range of ω and ρ before its predictions become more significant than the fluctuations [25]. This limitation is manifest for instance, in the fact that $n_{F,\omega}(\tau^-)$ is not positive definite, whereas $n_F^\pm(\tau^-)$ and $(\beta\beta^\dagger)_{\omega\omega,F}$ are positive definite.

Equation (45), together with (43), specifies the distribution $n_{F,\omega}(\tau^-)$ anywhere in the spacetime directly in terms of the observer's rapidity. Similarly, the spatial distribution of backward-moving particles/antiparticles is given by:

$$n_B^\pm(\tau, \rho) = \int_0^{\infty} \frac{d\omega}{2\pi} \int_0^{\infty} \frac{d\omega'}{2\pi} (\beta\beta^\dagger)_{\omega\omega',B} e^{i(\omega' - \omega)\tau^+} \quad (47)$$

$$= \frac{1}{4\pi^2} \int_{-\infty}^{\infty} \frac{d\tau}{\tau} g_-(\tau^+ + \tau, \tau) = \int_0^{\infty} \frac{d\omega}{2\pi} n_{B,\omega}(\tau^+) \quad (48)$$

where

$$n_{B,\omega}(\tau^+) = \frac{2}{\pi^2} \int_{-\infty}^{\infty} d\tau_a \frac{\sin[2\omega(\tau^+ - \tau_a)]}{\tau^+ - \tau_a} \int_0^{\infty} d\tau_d \sin(2\omega\tau_d) g_-(\tau_a, \tau_d) \quad (49)$$

Clearly the backward moving particle content (which exactly matches the backward moving antiparticle content) is a function only of $\tau^+ = \tau + \rho$.

Although the distributions of 'forward'- and 'backward'-moving particles are not generally the same, we might expect them to be related when the observer's trajectory is time-symmetric. To study this possibility, consider an observer whose trajectory satisfies the time-reversal symmetry

$$\begin{aligned} x_\lambda(-\tau_\lambda) &= x_\lambda(\tau_\lambda) \\ t_\lambda(-\tau_\lambda) &= -t_\lambda(\tau_\lambda) \end{aligned} \quad (50)$$

It follows that $\alpha(-\tau_\lambda) = -\alpha(\tau_\lambda)$, which gives $n_{F,\omega}(\tau') = n_{B,\omega}(-\tau')$ for all τ' . On the hypersurface $\tau = 0$, for instance, where $\tau^\pm = \pm\rho$, this implies that the distribution of

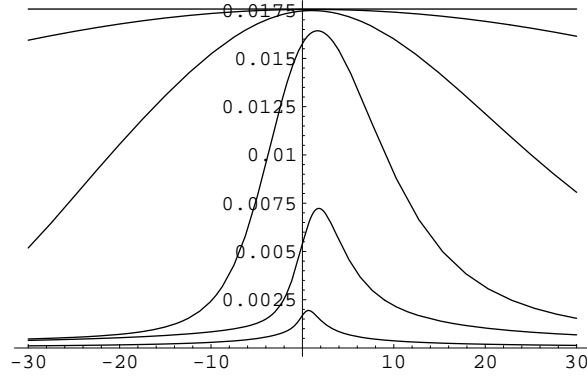


Figure 5. $n_{F,B}(\rho)/a$ for the smooth turnaround observer, as a function of $a\rho$ for $\tau = 0$ and $a\tau_c = 1$ (bottom curve), 3, 10, 30, 100 and ∞ (top curve).

forward moving particles exactly matches that of backward moving particles. However, on the observer's worldline, the distribution of forward moving particles is the time-reverse of the distribution for backward moving particles.

4. Examples

4.1. Inertial Observer

For an inertial observer, α is constant, which gives $g_{\pm}(\tau_a, \tau_d) = 0$. The particle content is therefore everywhere zero, as expected.

4.2. Constant Acceleration

For a uniformly accelerating observer we have

$$g_{+}(\tau_a, \tau_d) = g_{-}(\tau_a, \tau_d) = \frac{1}{2\tau_d} - \frac{a}{2\sinh(a\tau_d)}$$

which is independent of τ_a . Hence the forward and backward moving particle distributions are both uniform w.r.t. ρ for all τ , and the frequency distribution is everywhere given by:

$$n_{F,\omega} = n_{B,\omega} = \frac{1}{\pi} \int_0^{\infty} d\tau_d \sin(2\omega\tau_d) \left(\frac{1}{\tau_d} - \frac{a}{\sinh(a\tau_d)} \right) \quad (51)$$

$$= \frac{1}{1 + e^{\frac{2\pi\omega}{a}}} \quad (52)$$

which is a thermal spectrum at temperature $T = \frac{a}{2\pi k_B}$, as expected [8, 3, 26].

4.3. A 'Smooth Turnaround' Observer.

Consider again the observer with acceleration

$$a(\tau_{\lambda}) = a \cosh^{-2} \left(\frac{\tau_{\lambda}}{\tau_c} \right)$$

By substituting the corresponding rapidity $\alpha(\tau_\lambda) = a\tau_c \tanh(\tau/\tau_c)$ into equation (43), we immediately obtain the spatial distribution of forward or backward moving particles. At time $\tau = 0$ these distributions are equal, as a result of the time-reversal invariance of the observer's trajectory. They are shown in Figure 5 as a function of $a\rho$ for $a\tau_c = 1$ (bottom curve), 3, 10, 30, 100 and ∞ (top line). As τ_c increases the particle density increases, and approaches the spatial uniformity found for the 'constant-acceleration' ($\tau_c \rightarrow \infty$) limit.

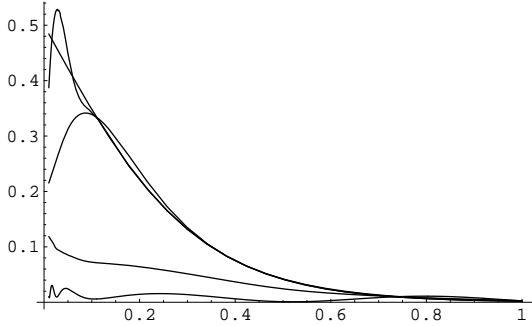


Figure 6(A). $n_{F,\omega}(\rho)$ for the smooth turnaround observer, as a function of ω/a for $\rho = 0 = \tau$, and $a\tau_c = 3, 10$ and 30 .

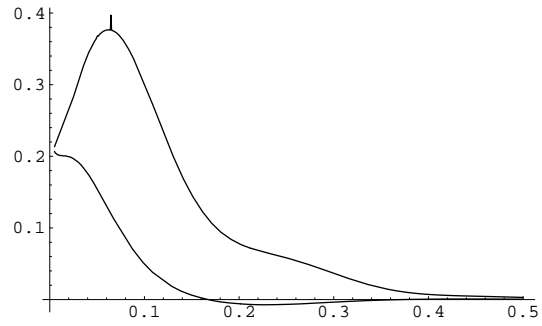


Figure 6(B). $n_{F,\omega}(\rho)$ for the smooth turnaround observer, as a function of ω/a for τ , $a\tau_c = 10$ and $a\rho = \pm 10$.

Figure 6 shows the frequency distribution $n_{F,\omega}(\rho)$ of forward-moving particles as a function of ω/a for $\tau = 0$. (This also equals the backward-moving distribution $n_{B,\omega}(\rho)$ there.) In Figure 6 (A) we have $\rho = 0$ and $a\tau_c = 3, 10, 30$ and ∞ . We see clearly that the distribution approaches the thermal form as τ_c increases, with only the low frequencies differing significantly from the constant acceleration case. In Figure 6 (B), $a\tau_c = 10$ and $a\rho = +10$ (top curve) and -10 (bottom curve). Since $n_{F,B}$ depend only on τ^+ and τ^- respectively, Figure 6 (B) also represents the distribution of forward/backward moving particles on the observer's worldline, at $\tau_\lambda = 10/a$. At this time the observer sees more backward moving particles than forward moving particles, while the forward/backward moving distributions are the opposite at $\tau = -10/a$.

4.4. Acceleration at Late Times.

Consider again the observer of Section 2.4, whose worldline is shown in Figure 3, in the (x, t) and (ρ, τ) planes. Figure 7 shows the spatial distribution of forward and backward moving particles on this observer's trajectory. On the trajectory the observer consistently sees more forward than backward moving particles. Since $n_{F,B}$ depend only on τ^+ and τ^- respectively we can again extrapolate from Figure 7 to the whole (ρ, τ) plane. Well into region F (see Figure 3 (B)) the forward/backward distributions are approximately uniform, in agreement with the predictions of the constant acceleration case. In region L there are many forward moving particles but few backward movers. In region R there are many backward moving particles but few forward movers, while in region P, where the observer is almost inertial, few particles of any variety will be

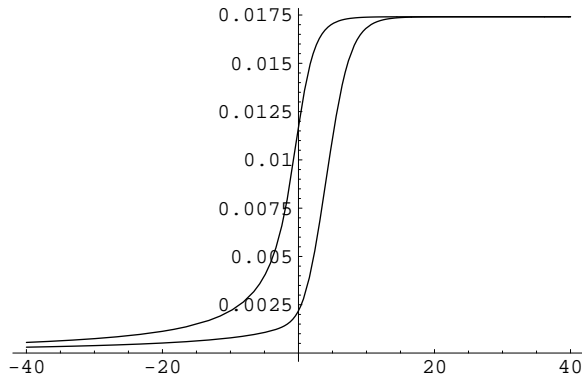


Figure 7. $n_F(\tau)/a$ (top) and $n_B(\tau)/a$ (bottom) for the ‘late-time acceleration’ observer as a function of $a\tau$ for $\rho = 0$ and $a\tau_c = 1$.

observed. The distributions $n_{F,B}(\tau)$ of Figure 7 can be decomposed into their frequency components by plotting $n_{B,\omega}(\tau)$ and $n_{F,\omega}(\tau)$ for various values of ω . This is done in Figure 8 for $\omega/a = 0.05$ (A) and 0.5 (B).

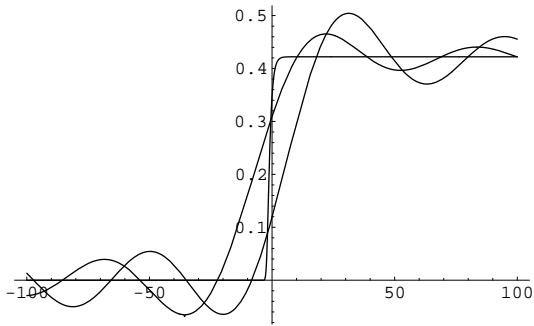


Figure 8(A). $n_{F,\omega}(\tau)$ and $n_{B,\omega}(\tau)$ for the ‘late-time acceleration’ observer as a function of $a\tau$ for $\rho = 0$, $\omega/a = 0.05$ and $a\tau_c = 1$.

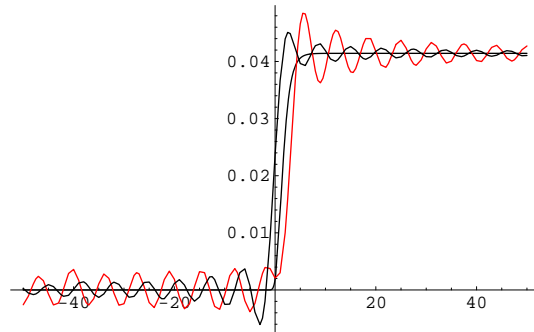


Figure 8(B). $n_{F,\omega}(\tau)$ and $n_{B,\omega}(\tau)$ for the ‘late-time acceleration’ observer as a function of $a\tau$ for $\rho = 0$, $\omega/a = 0.5$ and $a\tau_c = 1$.

These plots clearly show that $n_{F,\omega}(\tau)$ and $n_{B,\omega}(\tau)$ are not positive definite, despite the positive definiteness of $n_{F,B}(\tau)$. Also included in Figure 8 are the predictions obtained from the naive ‘instantaneous thermal spectrum’ $2\pi/(1 + e^{2\pi\omega/a(\tau)})$ that would result from substituting $a(\tau)$ directly into equation (52). The high frequency modes, which probe only short distance scales, closely trace these naive predictions, whereas the low frequency modes take more time to adjust from the ‘inertial’ to the ‘uniform acceleration’ predictions.

Figure 9 shows $n_{F,\omega}(\tau)$ and $n_{B,\omega}(\tau)$ as a function of ω/a , for $\tau = -30/a, 0$ and $30/a$. At late times the spectrum is close to thermal. For $\tau = 0$ neither the forward (Figure 9 (B)) nor backward (Figure 9 (A)) moving distributions resemble a thermal spectrum, even at large frequencies, and $n_{B,\omega}(\tau)$ is not positive definite. At much earlier times both distributions are very small, and neither is positive definite. The limit as $\omega \rightarrow 0$ of these distributions is independent of τ , reflecting the fact that the $\omega = 0$ mode is a global feature. However, this limit is different for forward and backward moving

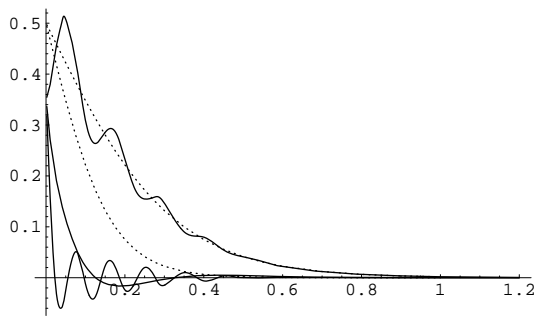


Figure 9(A). $n_{B,\omega}(\tau)$ for the ‘late-time acceleration’ observer, as a function of ω/a , for $\rho = 0$, $a\tau_c = 1$ and $a\tau = -30, 0$ and 30 . Also included are the ‘instantaneous thermal spectrum’ predictions $(1 + e^{2\pi\omega/a(\tau)})^{-1}$ (dotted).

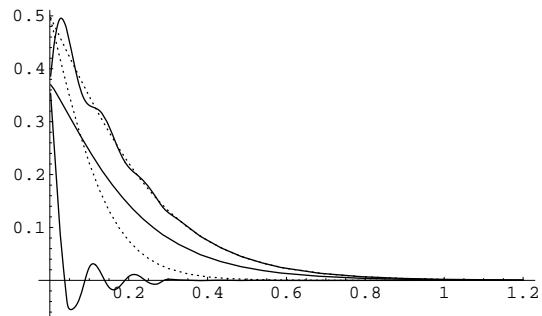


Figure 9(B). $n_{F,\omega}(\tau)$ for the ‘late-time acceleration’ observer, as a function of ω/a , for $\rho = 0$, $a\tau_c = 1$ and $a\tau = -30, 0$ and 30 . Also included are the ‘instantaneous thermal spectrum’ predictions $(1 + e^{2\pi\omega/a(\tau)})^{-1}$ (dotted).

particles.

5. Discussion

The approach developed in [17, 19, 25] has been used to evaluate the particle content of the massless Dirac vacuum for an arbitrarily moving observer in 1+1 dimensions. This method uses Bondi’s ‘radar time’, which provides a foliation of flat space that depends only on the observer’s trajectory. It agrees with proper time on the trajectory, and is single valued in the causal envelope of the observer’s worldline.

The particle content can be described in terms of ‘forward moving’ particles (with particle density $n_F^+(\tau, \rho)$ dependent only on $\tau - \rho$), ‘backward moving’ particles (with particle density $n_B^+(\tau, \rho)$ dependent only on $\tau + \rho$), and their corresponding antiparticles (described by n_F^- and n_B^-). The calculation of $n_{B,F}^\pm(\tau, \rho)$ is largely independent of the possible presence of horizons, although when horizons exist an observer cannot assign particle/antiparticle densities to regions of spacetime invisible to this observer. This is entirely reasonable, though it differs from other approaches [15]. The particle content is clearly different for different observers, but for any given observer the total number of forward/backward moving particles is independent of τ . This result is specific to massless particles in 1+1 dimensions, and is a direct consequence of conformal invariance. The spatial distribution of forward moving particles always matches that of forward moving antiparticles, and likewise for backward moving particles. In general, there is no connection between the observed numbers of forward moving particles and backward moving particles. However, when the observer’s trajectory is time-reversal invariant, the distribution of forward and backward moving particles must match at $\tau = 0$. Their distributions at other times is then specified by the fact that $n_F^\pm(\tau, \rho)$ depends only on $\tau - \rho$ and that $n_B^\pm(\tau, \rho)$ depends only on $\tau + \rho$.

These general results have been illustrated by four examples. We have confirmed

that inertial observers do not observe particles in the inertial vacuum, and that uniformly accelerating observers measure the well-known Fermi-Dirac spectrum [3, 4, 5, 6, 7, 8, 10, 25, 26]. This thermal spectrum is spatially uniform in ‘radar distance’ ρ and is the same for forward and backward moving particles, as expected. An observer with acceleration $a(\tau_\lambda) = a \cosh^{-2}(\tau/\tau_c)$ has also been studied. For large τ_c , this observer increasingly resembles the uniformly accelerating observer, although no horizons are present. For $|\rho|, |\tau| \ll \tau_c$ the particle content measured by this observer closely resembles the uniformly accelerating case, particularly for high frequency modes, which probe only short distance scales. This sheds light on a common misconception – that the Unruh effect is “due to the presence of a horizon”. As a result of the time-reversal invariance of this example, we find $n_F^\pm(0, \rho) = n_B^\pm(0, \rho)$ for all ρ as generally predicted, although $n_F^\pm(\tau, \rho) \neq n_B^\pm(\tau, \rho)$ for $\tau \neq 0$.

The further example treated here is an observer with $a(\tau_\lambda) = \frac{a}{1+e^{(\tau/\tau_c)}}$. This observer accelerates uniformly at late times, but is inertial at early times. The observed particle content closely resembles the uniform acceleration result in the causal future of the acceleration, but approaches zero at early times (and away from the horizon). The distributions of forward and backward moving particles now differ significantly, with $n_F^\pm(\tau, 0) > n_B^\pm(\tau, 0)$ for all τ . This intriguing result suggests an observer-dependent violation of discrete symmetries, which calls for further investigation.

Since massless fermions in 1+1 dimensions are conformally invariant, and consequently lack the scale dependence of the massive case (provided for instance by the Compton scale $1/m$). The results obtained here will not generalize immediately to massive particles, or to 3+1 dimensions. Further work is needed to investigate those cases in more detail, and to explore the possible observer dependence of discrete symmetries.

6. References

- [1] W. G. Unruh, *Phys. Rev. D* **14** (1976), 870 - 892.
- [2] P.C.W. Davies, *J. Phys. A.* **8(4)** (1975), 609 - 616.
- [3] M. Soffel, B. Müller and W. Greiner, *Phys. Rev. D* **22** (1980), 1935 - 1937.
- [4] R. J. Hughes, *Annals. Phys.* **162** (1985), 1 - 30.
- [5] P. Candelas and D. Deutsch, *Proc. R. Soc. London Ser. A.* **362** (1978), 251 - 262.
- [6] B. R. Iyer and A. Kumar, *J. Phys. A.* **13** (1980), 469 - 478.
- [7] S. Hacyan, *Phys. Rev. D.* **33(12)** (1986), 3630 - 3633.
- [8] S. Takagi, *Prog. Theo. Phys. Supplement No.* 86, 1986.
- [9] N.D. Birrell and P.C.W. Davies, *Quantum Fields in Curved Spacetime* (Cambridge University Press, 1982).
- [10] M. Horibe, *Prog. Theor. Phys.* **61(2)** (1979), 661 - 671.
- [11] L. Sriramkumar and T. Padmanabhan, *Class. Quantum Grav.* **13** (1996), 2061 - 2079.
- [12] N. Sanchez, *Phys. Lett. B.* **105(5)** (1981), 375 - 380.
- [13] N. Sanchez, *Phys. Lett. B.* **87(3)** (1979), 212 - 214.
- [14] N. Sanchez, *Phys. Rev. D.* **24(8)** (1981), 2100 - 2110.
- [15] Zhu Jian-yang, Bao Aidong and Zhao Zheng, *Intl. J. Theoret. Phys.* **34(10)** (1995), 2049 - 2059.
- [16] N. Sanchez and B. F. Whiting, *Phys. Rev. D.* **34(4)**, (1986), 1056 - 1071.

The Fermionic Particle Density of Flat 1+1 Dimensional Spacetime seen by an Arbitrarily Moving Observer

- [17] C. E. Dolby, 'A State-Space Based Approach to Quantum Field Theory in Classical Background Fields', Thesis, Geometric Algebra Research Group, Cambridge University.
- [18] C. E. Dolby and S. F. Gull, *Am. J. Phys.* **69**, (2001), 1257 - 1261.
- [19] C. E. Dolby and S. F. Gull, *Annals. Phys.* **293** (2001), 189 - 214.
- [20] C. W. Misner, K. S. Thorne and J. A. Wheeler, *Gravitation* (Freeman 1973).
- [21] M. Pauri and M. Vallisneri, *Found. Phys. Lett.* **13**(5) (2000), 401 - 425.
- [22] H. Bondi, *Assumption and Myth in Physical Theory* (Cambridge University Press, 1967).
- [23] D. Bohm, *The Special Theory of Relativity* (W. A. Benjamin, 1965).
- [24] R. D'Inverno, *Introducing Einstein's Relativity* (Oxford University Press, 1992).
- [25] C. E. Dolby and S. F. Gull, 'Radar Time and a State-Space Based Approach to Quantum Field Theory in Gravitational and Electromagnetic Backgrounds', preprint number gr-qc/0207046.
- [26] W. Greiner, B. Müller and J. Rafelski, *Quantum Electrodynamics of Strong Fields, with an Introduction to Modern Relativistic Quantum Mechanics*, section 21 (Springer-Verlag, 1985).